

- [15] The tight-binding calculations used an extended Hückel-type Hamiltonian (M.-H. Whangbo, R. Hoffmann, *J. Am. Chem. Soc.* **1978**, *100*, 6093). The off-diagonal matrix elements of the Hamiltonian were calculated according to the modified Wolfsberg–Helmholz formula (J. Ammeter, H.-B. Bürgi, J. Thibeault, R. Hoffmann, *J. Am. Chem. Soc.* **1978**, *100*, 3686). A basis set composed of double- ζ Slater-type orbitals for C and S and single- ζ Slater-type orbitals for H was used. The exponents, contraction coefficients, and atomic parameters were taken from previous work [14].
- [16] S. Horiuchi, H. Yamochi, G. Saito, K. Sakaguchi, M. Kusunoki, *J. Am. Chem. Soc.* **1996**, *118*, 8604.
- [17] The temperature dependence of the resistance was measured using the standard four-probe DC method down to 10 K as well as the AC technique down to 0.5 K using a ^3He system. Contacts with four annealed platinum wires (20 μm in diameter) to the surface of the sample were made with a conductive graphite paste.
- [18] H. H. Wang, B. A. Vogt, U. Geiser, M. A. Beno, K. D. Carlson, S. Kleinjan, N. Thorup, J. M. Williams, *Mol. Cryst. Liq. Cryst.* **1990**, *181*, 135.

Efficient Energy Transfer from Blue to Red in Tetraphenylporphyrin-Doped Poly(9,9-dioctylfluorene) Light-Emitting Diodes**

By Tersilla Virgili, David G. Lidzey, and Donal D. C. Bradley*

Light-emitting diodes (LEDs) based on conjugated polymers offer significant potential advantages over other competing technologies, as they can be fabricated cheaply and easily by solution-based processing techniques. The operational lifetime and power efficiency of such devices have now reached a point where commercial products can be expected soon.^[1] Initial applications are likely to be in monochrome back-lights for liquid crystal displays in mobile phones followed by monochrome pixelated displays in the same devices. Full-color red–green–blue (RGB) displays based on organic materials are a very attractive prospect, and a number of routes to fabricate such devices have been suggested.^[2–6] One of the most exciting prospects is the use of ink-jet printing technology to allow direct patterning of conjugated-polymer LED pixels.^[6] The first report described the use of a single polymer in a monochrome display but full-color prototypes have also been recently reported.^[7]

In general, the emission spectra of conjugated polymers have a large full width at half maximum, FWHM \approx 50 to

100 nm. This is due to both inhomogeneous broadening and the presence of a vibronic progression. For RGB displays, however, saturated colors are needed to achieve a full color palette. We report here on the development of a saturated-red-emitting system suitable for use in LED displays. Our approach is to dope the fluorescent red dye tetraphenylporphyrin (TPP) into the blue light-emitting conjugated polymer poly(9,9-dioctylfluorene), PFO. This and other polyfluorenes are under intense investigation for application in state-of-the-art LEDs.^[7–11] In our system one can combine the inherent advantages of ease of device fabrication for a solution-based conjugated polymer with the narrow emission linewidth and red spectral characteristics of the TPP dye. The resulting demonstration of efficient single-step Förster transfer from blue to red uses the specific properties of porphyrins, namely their possession of a high oscillator strength Soret band absorption in the blue, which is efficiently coupled to the strongly spectrally displaced Q-band red emission. The use of dopants, including TPP,^[12] to change emission wavelength is well documented and has been exploited in LEDs based on sublimed molecular materials. Similar approaches have also been used, but to a substantially lesser extent, for conjugated-polymer LEDs. For example, Tasch et al.^[13] have used combinations of the blue-emitting ladder polymer poly(*p*-phenylene) as host with polymers containing a perylene moiety as guest. In these devices, orange-red emission occurred from the guest material but the linewidth was still broad. Thus, whilst other groups have previously used a variety of dopants to energy-shift emission via Förster transfer, we demonstrate here an exceptionally large shift using a single-step transfer to obtain a saturated red emission. This is potentially important for applications since it allows a single material to be used as a blue light emitter, as a host for green emission dyes, and as a host for a red emission dye. This may simplify processing of full-color display pixels, especially via ink-jet and other printing schemes, where the existence of a common component should assist ink formulation.

Figure 1a shows the absorption and photoluminescence (PL) emission spectra of TPP (the chemical structure of which is also shown). The porphyrin “Soret” band appears as a strong narrow absorption that peaks at 418 nm. The two weaker absorptions with peaks at 512 nm and 550 nm are the Q-bands, also typical of porphyrins. The PL spectrum shows two sharp transitions at 653 nm and 714 nm. Figure 1b shows the corresponding data for PFO. The PL emission from PFO extends from 400 nm to 600 nm with clear vibronic peaks at 423 nm (0–0) and 441 nm (0–1) and a shoulder at 468 nm (0–2). There is a strong overlap of the PFO 0–0 emission peak with the Soret band absorption of TPP such that efficient Förster transfer can be anticipated.^[14] Direct emission from the TPP Soret band is very weak but efficient internal conversion to the Q-band results in the characteristic red emission. Förster transfer can also take place between the long-wavelength tail of the PFO emission (resulting from interchain interactions^[15])

[*] Prof. D. D. C. Bradley, Dr. D. G. Lidzey, T. Virgili
Department of Physics and Astronomy & Centre for Molecular
Materials
The University of Sheffield
Hicks Building, Hounsfield Road, Sheffield S3 7RH (UK)

[**] We thank Dr. Mike Inbasekaran, Dr. Ed Woo, and Dr. Weishi Wu of The Dow Chemical Company for providing the poly(9,9-dioctylfluorene) and BFA samples used in these experiments. We also thank Robert Fletcher for assistance with device fabrication and Dr. Alasdair Campbell for helpful discussions. DGL thanks the Lloyd's of London Tercentenary Fund for provision of a Research Fellowship. We also thank the Engineering and Physical Sciences Research Council of the UK for financial support (grant GR/M45115).

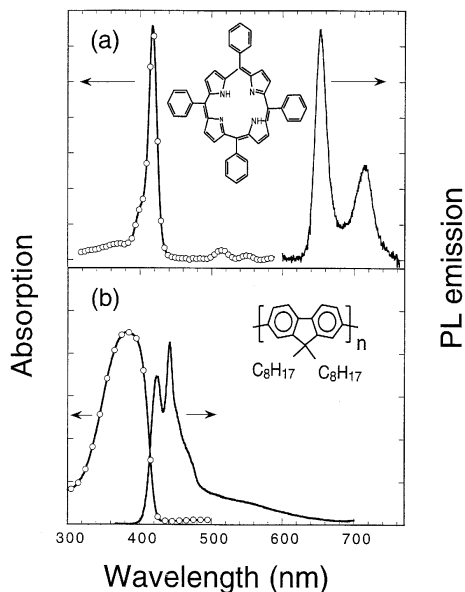


Fig. 1. a) The absorption and PL emission spectra from a film of TPP doped into a PMMA host matrix at 5 wt.-% concentration. The chemical structure of TPP is also shown. b) The absorption and PL emission spectra from a thin film of poly(9,9-dioctylfluorene) (PFO). The chemical structure of PFO is also shown.

and the Q-band absorption, although in this case the normalized overlap is quite small. Blending the red-emitting TPP into the blue-emitting PFO should thus red-shift the emission from a peak at 441 nm to a peak at 653 nm. Moreover, since the human eye has very little sensitivity beyond 700 nm,^[16] the TPP vibronic replica at 714 nm is not seen. The emission spectrum thus changes from a broad-band whitish blue (Commission Internationale de l'Eclairage (CIE) (1931) coordinates $X = 0.20$, $Y = 0.15$) to a narrow red peak ($X = 0.65$, $Y = 0.29$).

Figure 2 shows the $\lambda = 354$ nm excited PL emission from PFO/TPP blend films with TPP concentrations (by weight) of 0.08 %, 0.15 %, and 1 %. At the lowest TPP concentrations, the blue PFO emission (peaking at 447 nm) dominates the PL spectrum. As the TPP concentration is increased, its characteristic red emission grows at the expense of the PFO emission. At 1 %, virtually no emission is observed from the PFO, and the TPP emission component completely dominates.

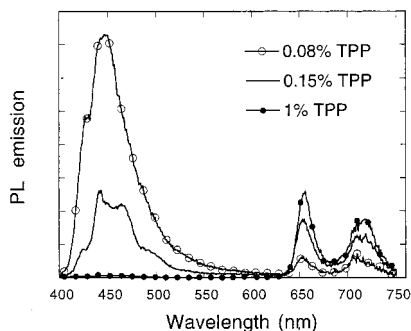


Fig. 2. The PL emission from TPP/PFO blend films at different TPP concentrations (by weight) following optical excitation at 354 nm.

PFO blend film, we find that the absorption coefficient of the blend film is approximately 1 % greater than that of the control. This indicates that, for the blend at this concentration, at least 99 % of the photons are absorbed by the PFO. The emission is, however, dominated by the TPP, a result that confirms efficient Förster transfer from the PFO.

We have determined the PL quantum efficiency of PFO and TPP using our calibrated integrating sphere. For the thin films of PFO (following direct excitation at 354 nm) used here we find a PL quantum efficiency of (46 ± 4) %. To measure the PL quantum efficiency of TPP by direct excitation at 354 nm, it is necessary to create films with a relatively large optical absorption coefficient *at the excitation wavelength*. This minimizes systematic errors in the measurement that otherwise cause underestimates of the PL efficiency. TPP samples were prepared by dispersing TPP in an inert poly(methylmethacrylate) (PMMA) matrix at a concentration of 5 wt.-%. Relatively thick (~350 nm) films of TPP/PMMA were cast from solution and had an absorption of approximately 30 % at 354 nm. With these samples, we determine the quantum efficiency for TPP to be (10 ± 1) %. For a 1 % TPP/PFO blend film (where more than 99 % of the excitation photons are absorbed by the PFO) we determine a total quantum efficiency of 9.5 %. This indicates that at least 95 % of the excitons photogenerated in PFO are Förster-transferred to the TPP.

Figure 3 shows the PL quantum yields for the TPP and PFO emission components of the spectra as a function of

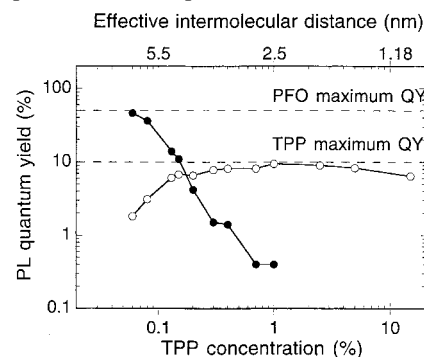


Fig. 3. The PL quantum yield [%] of the TPP red emission (empty circles) and of the PFO blue emission (filled circles) for different concentrations (by weight) of TPP in the blend. The upper x-axis scale shows the average TPP intermolecular distance.

TPP concentration in the blend film. These were calculated by integrating the emission over the range 400–600 nm for PFO and the range 620–760 nm for TPP. On the upper x-axis the effective distance (d) between TPP molecules is given. This distance was calculated assuming that the TPP molecules are uniformly dispersed throughout the blend film, with each molecule occupying a volume of $(4/3)\pi d^3$. Below a 1 wt.-% concentration the TPP quantum yield decreases, reaching a value of 1.5 % at a 0.06 wt.-% concentration. The reduction in emission from the TPP is due to an increase in the effective average distance between an exciton located on a PFO chain segment and a TPP molecule. This leads to a reduction in the dipole–dipole cou-

pling between the donor and acceptor, increasing the effective probability that the exciton will radiatively decay on a PFO chain segment rather than transfer to a TPP molecule. Above a 0.4 wt.-% concentration, the TPP PL quantum yield is approximately constant at $(9 \pm 1) \%$ until, at concentrations greater than 5 %, the quantum yield again reduces, reaching a value of 6.5 % at a TPP weight concentration of 11 %. The reduction of quantum yield at high dopant concentrations is believed to be due to intermolecular interactions between the TPP molecules, leading to new non-radiative decay channels possibly involving molecular excimers.^[17]

The concentration dependence has been analyzed in terms of a dipole–dipole Förster transfer from the PFO to TPP. The Förster radius (R_0) is defined as the distance between the donor and the acceptor at which the probability of intermolecular energy transfer equals that for relaxation of the donor by fluorescence. This effectively means that an exciton is as likely to decay (either radiatively or non-radiatively) on a TPP molecule as it is to decay on a PFO molecule. However, as the quantum yield of fluorescence for PFO is approximately 4.6 times greater than for TPP, the Förster transfer radius is identified as the average intermolecular distance at which the fluorescence quantum yield from PFO is ~ 4.6 times greater than that of TPP. This condition occurs at a TPP intermolecular distance of 5.4 nm (corresponding to a weight concentration of 0.107 %). Here, the quantum efficiency of emission from PFO is 22.7 %, and from TPP it is 4.8 %.

R_0 can also be calculated from the relative overlap of the donor emission and acceptor absorption spectra.^[12] The expected relation is

$$(R_0)^6 = \frac{0.5291 K^2}{N_A n^4} T \quad (1)$$

where K^2 is an orientation factor ($2/3$ for random orientation), N_A is Avogadro's number, and n is the refractive index of the host. T is the overlap integral between the absorption spectrum of the acceptor and the fluorescence spectrum of the donor and is defined by

$$T = \int_0^{\infty} F_m(\bar{\nu}) \varepsilon_Q(\bar{\nu}) \frac{d\nu}{\bar{\nu}^4} \quad (2)$$

where F_m is the normalized fluorescence spectrum of the donor, and ε_Q is the molar decadic extinction coefficient of the acceptor, both expressed as a function of energy in wavenumbers ($\bar{\nu}$). For our TPP/PFO system, we calculate a value of $R_0 = 4.8$ nm. Using the same method, Shoustikov et al.^[12] have previously determined a Förster radius for energy transfer from an Alq₃ (tris(8-hydroxyquinoline) aluminum) donor to a TPP acceptor of 3.3 nm. The difference between these values occurs because the overlap between the emission spectrum of PFO and the absorption spectrum of TPP is 9 times greater than that for Alq₃ as donor. The larger value of T is reflected in an increase in the Förster transfer radius by a factor of $9^{1/6} = 1.44$. The increase in Förster transfer ra-

dius translates to a lower loading of the dye being required. High dye concentrations often lead to problems with phase separation and crystallization but they are not needed here. This behavior can be explained as a consequence of our utilization of the very high extinction coefficient TPP Soret band transition. For Alq₃ the spectral overlap of the emission is with the weaker Q-band transitions.

The fact that we determine a Förster radius from our quantum yield measurements that is larger (5.4 nm) than expected from a simple consideration of the overlap of absorption and emission spectra (4.8 nm) suggests the need for further consideration of the processes involved in dipole–dipole transfer between extended polymer chain segments and localized dye molecules. In particular the wavefunction of an exciton located upon a conjugated polymer chain can be delocalized over a number of monomer units and thus has a greater spatial extent than an exciton located upon a dye molecule. Moreover, an exciton on a conjugated polymer chain is able to diffuse along the chain, and also hop between chains. It has been estimated that in the polymer poly(*p*-phenylene vinylene)^[18] this distance can be up to 8 nm. Thus the value of R_0 calculated by a simple dipole–dipole coupling between two localized states would always be expected to underestimate the transfer radius of the composite system.^[19]

Figure 4 shows a plot of the current density as a function of applied device bias for an ITO/BFA/(TPP/PFO)/Ca

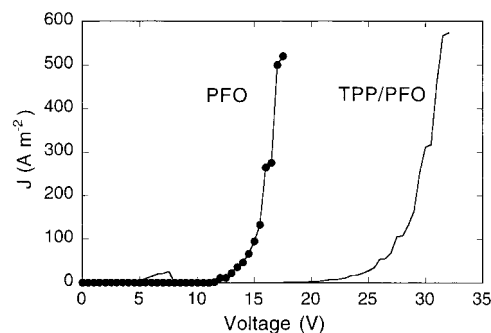


Fig. 4. Current density J (as a function of applied device bias) for a PFO LED (filled circles) and for an LED otherwise identical to the emissive PFO device but doped with 2.5 wt.-% TPP (solid line).

LED, where ITO is indium tin oxide and BFA is a copolymer (see Fig. 5 and the Experimental section). The device turns on at 20 V (arbitrarily defined as the bias required to give a measurable luminance of 1 cd m^{-2}) with a corresponding current density of $J = 2.5 \text{ A m}^{-2}$. At an applied voltage of 33 V ($J = 600 \text{ A m}^{-2}$), we measure a luminance of 90 cd m^{-2} . The EL emission from the device is identical

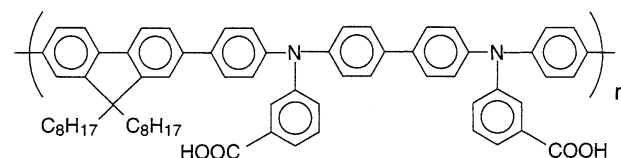


Fig. 5. The chemical structure of the hole transport polymer BFA.

to the PL emission from the TPP (see Fig. 1a) and has CIE (1931) coordinates $X = 0.65$ and $Y = 0.29$, i.e., a good red.^[16] We calculate an external EL quantum efficiency at 33 V of 0.9 %, corresponding to 0.18 cd/A. This is a large value for a red emission material. Equivalent, optimized PFO LEDs without the TPP have an EL quantum efficiency of 0.2 % (0.25 cd/A).^[9] Although the EL quantum yield of the TPP-doped LED is nearly five times higher than that with PFO alone, the luminance efficiency of the TPP-doped device in candela per amp is reduced. This is simply a consequence of the reduced sensitivity of the eye to red light compared to blue.^[16]

Simple arguments based on the generation rate of singlet excitons^[20] within an organic LED suggest that

$$\Phi_{\text{EL}} = \Phi_{\text{PL}} \eta \gamma \quad (3)$$

where Φ_{EL} is the EL quantum efficiency, Φ_{PL} is the PL quantum efficiency, η is the spin factor for singlet exciton generation, and γ is a charge balance factor determining the overall exciton generation rate. Hence the observed reduction in the PL quantum yield of the TPP/PFO blend film (≈ 10 %) compared to PFO on its own (≈ 50 %) might have been expected (with all other factors remaining constant) to reduce the EL quantum yield by a factor of at least five. However, the PFO/TPP blend device has an EL quantum yield which is five times higher than for the undoped PFO device. There is thus a discrepancy in the expected EL quantum yield by a factor of 25. We propose that the charge balance factor γ increases in the doped devices, with the result of an increased exciton generation rate. As the TPP molecules have a HOMO–LUMO energy separation that is smaller than that of PFO, they could act as efficient charge traps. It has been shown that PFO devices are injection limited^[21] and that the current flowing through such devices is dominated by holes, which have a high mobility.^[8] The introduction of hole traps would allow the formation of a positive space charge, which could lead to a reduction in the hole current and an enhanced electron injection. The charge balance factor γ would then increase. Time-of-flight mobility measurements for hole transport do indeed show a large drop in mobility for the TPP-doped PFO in comparison to undoped PFO.^[22] An increased barrier to the injection of majority hole carriers into the LED is also indicated by an increase in the turn-on voltage of the TPP-doped devices compared to the pure PFO devices (see Fig. 4). As a consequence of such hole trapping, it is likely that direct recombination of electrons and holes can occur on individual TPP molecules. This could clearly also contribute to the increase in EL quantum yield. Similar observations of an increase in LED efficiency following doping have been reported by Tasch et al.^[13] for a polymer/polymer blend system.

The EL quantum efficiency of the TPP/PFO LEDs is comparable to, and in many cases larger than, that reported for other red LEDs. For example Burrows et al.^[3]

reported a TPP-doped Alq₃ LED with an efficiency of 0.07 %. Values of 0.5 % were obtained by Hu et al.^[23] for a dye-doped copolymer blend system emitting at ≈ 645 nm. Higher efficiencies have been reported for blends doped with phosphorescent compounds. Gu et al. reported an efficiency of 1.6 %^[4] and Baldo et al. reported 4 %.^[24] Note, however, that the doped systems in the latter devices remove the limitations on η since both triplet and singlet states can emit.

In conclusion, we have presented a system of a blue light-emitting host polymer (PFO) and a red light-emitting molecular guest molecule (TPP) suitable for use in solution-processable LEDs. The large overlap between the emission from the PFO and the Soret band of the TPP results in very efficient Förster transfer. A large Förster transfer radius $R_0 = 5.4$ nm is deduced. Between a TPP weight concentration of 1 and 10 %, we find that 95 % of photogenerated excitons are transferred from the PFO to TPP. Finally, in LED devices, we achieve external EL quantum efficiencies of 0.9 % at a luminance of 90 cd m⁻². The emission spectrum obtained has CIE (1931) coordinates $X = 0.65$ and $Y = 0.29$ and thus represents a good red.

Experimental

Poly(9,9-dioctylfluorene) (PFO) was synthesized at the Dow Chemical Company via a Suzuki coupling reaction [25] and was carefully purified to remove ionic impurities and catalyst residues. Tetraphenylporphyrin (TPP) was purchased from the Aldrich Chemical Company and was used without further purification. PFO was dissolved in toluene at a concentration of 20 mg/mL, and TPP was then added at concentrations (by weight) varying from 0.06 % to 15 %. Films of the TPP/PFO blend were prepared by spin-coating the solutions onto quartz substrates suitable for absorption and photoluminescence measurements. Films of TPP dispersed in poly(methyl-methacrylate) were also prepared as control samples.

Photoluminescence quantum efficiency measurements [26] were performed within a calibrated integrating sphere coupled via a fiber-optic link to a scanning monochromator with a photomultiplier as detector. The sample was mounted inside the sphere, and excited using the 354 nm line of a HeCd laser. The use of a monochromator to measure the light field within the sphere allows the relative contribution of the excitation and emission to be separated. Thus we determine the relative number of excitation photons inside the sphere (with the sample absent), and then with the sample present we measure the relative number absorbed by the sample. This is compared to the number of PL photons emitted by the sample, to give the fluorescence quantum efficiency. Excitation densities were deliberately kept low (≈ 0.5 mW cm⁻²) and all measurements were made under a nitrogen atmosphere to limit photo-oxidative degradation.

Double-layer LEDs were fabricated by first spin-coating a 50 nm layer of the hole-transporting polymer poly[9,9-dioctylfluorene-co-(bis-*N,N'*-(3-carboxyphenyl)-bis-*N,N'*-phenylbenzidine)] (BFA) onto (oxygen plasma cleaned) ITO-coated glass. The chemical structure of BFA is shown in Figure 5. On top of this layer, a solution of PFO having a dopant concentration of 2.5 % TPP was spin-coated, forming a 150 nm thick film. A calcium, electron-injecting cathode was then deposited onto the polymer films by thermal evaporation. All processing and device testing steps were made in a nitrogen-filled glove-box, containing a few parts-per-million background levels of water and oxygen. The LED brightness (as determined by the photopic response of the eye) was measured using a calibrated luminance meter. The external EL quantum efficiency of the devices was calculated by comparing the absolute luminance of the device in the forward direction to the current density flowing through the device, taking into account the spectral characteristics of the emitted light and the photopic efficiency of the detector [27].

Received: May 26, 1999
Final version: September 13, 1999

- [1] R. J. Visser, *Philips J. Res.* **1998**, *51*, 467.
 [2] D. G. Lidzey, D. D. C. Bradley, S. J. Martin, M. A. Pate, *IEEE J. Selected Top. Quantum Electron.* **1998**, *4*, 113.
 [3] P. E. Burrows, S. R. Forrest, S. P. Sibley, M. E. Thompson, *Appl. Phys. Lett.* **1996**, *69*, 1959.
 [4] G. Gu, G. Parthasarathy, S. R. Forrest, *Appl. Phys. Lett.* **1999**, *74*, 305.
 [5] C. C. Wu, J. C. Sturm, R. A. Register, M. E. Thompson, *Appl. Phys. Lett.* **1996**, *69*, 3117.
 [6] S. C. Chang, Y. Yang, R. Helgeson, F. Wudl, M. B. Ramey, J. R. Reynolds, *Appl. Phys. Lett.* **1998**, *73*, 2561.
 [7] H. Kobayashi, S. Kanbe, S. Seki, H. Kiguchi, M. Kimura, I. Yudasaka, S. Miyashita, T. Shimoda, C. R. Towns, J. H. Burroughes, R. H. Friend, in *Proc. of the 2nd Int. Conf. on Electroluminescence from Molecular Materials and Related Phenomena (ICEL'2)*, Sheffield, May **1999**; *Synth. Met.*, in press.
 [8] M. Redecker, D. D. C. Bradley, M. Inbasekaran, E. P. Woo, *Appl. Phys. Lett.* **1998**, *73*, 1565.
 [9] A. W. Grice, D. D. C. Bradley, M. T. Bernius, M. Inbasekaran, W. W. Wu, E. P. Woo, *Appl. Phys. Lett.* **1998**, *73*, 629.
 [10] M. Redecker, D. D. C. Bradley, M. Inbasekaran, W. W. Wu, E. P. Woo, *Adv. Mater.* **1999**, *11*, 241.
 [11] L. C. Palilis, D. G. Lidzey, M. Redecker, D. D. C. Bradley, M. Inbasekaran, E. P. Woo, W. W. Wu, *SPIE Proc.* **3797**, in press.
 [12] A. Shoustikov, Y. You, P. Burrows, M. E. Thompson, S. R. Forrest, *Synth. Met.* **1997**, *1*, 217.
 [13] S. Tasch, E. J. W. List, C. Hochfilzer, G. Leising, P. Schlichting, U. Rohr, Y. Geerts, U. Sherf, K. Müllen, *Phys. Rev. B* **1997**, *56*, 4479.
 [14] M. Pope, S. E. Swenberg, *Electronic Processes in Organic Crystals*, Clarendon, Oxford **1982**.
 [15] D. D. C. Bradley, M. Grell, X. Long, H. Mellor, A. W. Grice, M. Inbasekaran, E. P. Woo, *Proc. SPIE* **1997**, *3145*, 254.
 [16] G. A. Agoston, *Color Theory and Its Application in Art and Design*, Springer, Berlin **1979**.
 [17] E. Conwell, *Synth. Met.* **1997**, *85*, 1.
 [18] J. J. M. Halls, K. Pichler, R. H. Friend, S. C. Moratti, A. B. Holmes, *Synth. Met.* **1996**, *77*, 277.
 [19] U. Lemmer, A. Ochse, M. Deussen, R. F. Mahrt, E. O. Göbel, H. Bässler, P. Haring Bolivar, G. Wegmann, H. Kurz, *Synth. Met.* **1996**, *78*, 289.
 [20] R. H. Friend, R. W. Gymer, A. B. Holmes, J. H. Burroughes, R. N. Marks, C. Taliani, D. D. C. Bradley, D. A. Dos Santos, J. L. Brédas, M. Lögdlund, W. R. Salaneck, *Nature* **1999**, *397*, 121.
 [21] S. Janietz, D. D. C. Bradley, M. Grell, C. Giebeler, M. Inbasekaran, E. P. Woo, *Appl. Phys. Lett.* **1998**, *73*, 2453.
 [22] A. J. Campbell, private communication **1999**.
 [23] B. Hu, N. Zhang, F. E. Karasz, *J. Appl. Phys.* **1998**, *83*, 6002.
 [24] M. A. Baldo, D. F. O'Brien, Y. You, A. Shoustikov, S. Sibley, M. E. Thompson, S. R. Forrest, *Nature* **1998**, *395*, 151.
 [25] N. Miyaura, A. Suzuki, *Chem. Rev.* **1995**, *95*, 2457.
 [26] J. C. De Mello, H. F. Wittmann, R. H. Friend, *Adv. Mater.* **1997**, *9*, 230.
 [27] The external quantum yield (Φ_{EL}) is calculated using [28]

$$\Phi_{EL} = \frac{\pi e}{K_m hc J} \frac{L \int F(\lambda) d\lambda}{\int (1/\lambda) F(\lambda) y(\lambda) d\lambda} \quad (4)$$

where L is the luminance [cd m^{-2}] of the device at a current density of J [A m^{-2}], K_m is a conversion constant based on the maximum sensitivity of the eye (680 lm W^{-1}), $y(\lambda)$ is the normalized photopic spectral response function, $F(\lambda)$ is the EL spectrum, and λ is the wavelength.

- [28] D. F. O'Brien, *Ph.D. Thesis*, University of Sheffield, UK **1997**.

Preparation of Mesoporous High-Surface-Area Activated Carbon**

By Zhonghua Hu,* Madapusi P. Srinivasan, and Yaming Ni

Activated carbons (ACs) are usually microporous materials. Their main application is as adsorbents for the purification of gases and water, and chemical processing. According to the International Union of Pure and Applied Chemistry (IUPAC), the pores of a porous material can be classified into three groups: micropores (diameter, $d < 2 \text{ nm}$), mesopores ($2 \text{ nm} < d < 50 \text{ nm}$), and macropores ($d > 50 \text{ nm}$). For typical activated carbons, surface areas are $800\text{--}1500 \text{ m}^2/\text{g}$, mesopore surface areas are in the range of $10\text{--}200 \text{ m}^2/\text{g}$, and mesopore volumes vary between 0.1 and $0.2 \text{ cm}^3/\text{g}$, but higher values (up to $0.5 \text{ cm}^3/\text{g}$) can be found in special cases.^[1] The maximum of the pore volume distribution curve versus the pore width (diameter) is mostly in the range of $0.4\text{--}2.0 \text{ nm}$. The process of filling mesopores, also known as transitional pores, with adsorbate takes place via the mechanism of capillary condensation. Therefore, mesopores contribute significantly to adsorption, but also act as the main transport arteries for the adsorbate. In recent years, porous carbon materials have been used as catalytic materials, battery electrode materials, capacitor materials, gas storage materials, and biomedical engineering materials.^[2] For such applications, the carbon materials should have a high mesopore content, so that large molecules and ions that are too large to enter micropores can penetrate and be adsorbed efficiently in such pores. Microporous activated carbons, including ordinary AC, high-surface-area (HSA) AC, and carbon molecular sieves (CMS), have been extensively reported in the literature. In contrast, mesoporous activated carbons or mesoporous activated carbon fibers have been reported only recently.^[2-9] These mesoporous carbons, prepared via complicated and high-cost processes, usually have a low or moderate surface area.

CO_2 physical activation and ZnCl_2 chemical activation are two common methods for the production of activated carbon. It is also possible to combine the two processes.^[10,11] It was found that a simultaneous physical and

[*] Prof. Z. Hu, Prof. Y. Ni
 Department of Chemistry
 Tongji University
 1239 Siping Road, Shanghai 200092 (China)
 Dr. M. P. Srinivasan
 Department of Chemical Engineering
 National University of Singapore
 10 Kent Ridge Crescent, 119260 (Singapore)

[**] This work was supported by the National Science and Technology Board of Singapore (NSTB) under a grant for the project on Environmental Technology (RP 3602037) and the Scientific Research Foundation for Returned Overseas Chinese Scholars, State Education Ministry (China).